Biomaterials and Biosystems 17 (2025) 100107

Contents lists available at ScienceDirect

Biomaterials and Biosystems

journal homepage: www.elsevier.com/locate/bbiosy

Development of fully-resorption replacement paste-like organic/inorganic artificial bones compatible with bone remodeling cycles

Yuki Kamaya [a,1], Shiori Kato [a,1], Kazuaki Nakano [b], Masaki Nagaya [b], Hiroshi Nagashima [b,c], Mamoru Aizawa [a,d,*]

[a] Department of Applied Chemistry, School of Science and Technology, Meiji University, 1-1-1 Higashimita, Tama-ku, Kawasaki 214-8571, Kanagawa, Japan
[b] Meiji University International Institute for Bio-Resource Research (MUIIBR), 1-1-1 Higashimita, Tama-ku, Kawasaki 214-8571, Kanagawa, Japan
[c] Department of Life Sciences, School of Agriculture, Meiji University, 1-1-1 Higashimita, Tama-ku, Kawasaki 214-8571, Kanagawa, Japan
[d] Meiji University International Institute for Materials with Life Functions, Meiji University, 1-1-1 Higashimita, Tama-ku, Kawasaki 214-8571, Kanagawa, Japan

ARTICLE INFO

Keywords:
Paste-like artificial bone
β-tricalcium phosphate
Poly (lactic-co-glycolic acid) particles
Bone-forming ability
Bioresorbability
Bone remodeling cycle

ABSTRACT

Calcium-phosphate cement (CPC), commonly used as a bone graft substitute, sets as hydroxyapatite (HAp) and remains in the body for extended periods. To enhance bioresorbability, we developed a chelate-setting tricalcium β-phosphate (β-TCP) cement using inositol phosphate (IP6) surface modification. By incorporating poly (lactic-co-glycolic acid) (PLGA) particles as a pore-forming agent and calcium sulfate hemihydrate (CSH) to this CPC, we created an organic/inorganic hybrid cement combining bioresorbability with favorable material properties. In this study, varying amounts of PLGA particles were added alongside CSH, and the resulting cement's properties, cytotoxicity, and *in vivo* response large animals (pigs) were assessed. The cement exhibited a compressive strength of ~ 30 MPa and set within 15 min, making it suitable for clinical use. Cytotoxicity tests using Transwell® demonstrated cell growth in all cement specimens. In a pig tibia model, the amount of PLGA particle of 5 mass%, 10 mass%, and 20 mass% were tested to optimize material resorption and bone formation, compared with commercial HAp-based CPCs. Histological evaluations showed that higher amount of PLGA particles (10 mass% and 20 mass%) led to increased material resorption but impaired bone formation. The cement containing 5 mass% PLGA particles achieved the best balance, promoting the highest rate of bone formation. Thus, 5 mass% PLGA is the optimal amount for balancing resorption and bone regeneration in β-TCP cement. This formulation is expected to serve as a fully absorbable hybrid paste-type artificial bone supporting bone remodeling cycles.

1. Introduction

Worldwide, the number of people aged 65 years and over is increasing. As the number of elderly people increases, the number of patients with bone disease increases [1,2]. For example, osteoporosis is a common disease worldwide [3]. Osteoporosis is classified as primary or secondary. Primary osteoporosis occurs in postmenopausal women and people over 70 years of age due to aging [2]. Secondary osteoporosis can be caused by various factors, including disease, treatment, and lifestyle. Thus, osteoporosis can affect not only the elderly but also the younger generation. Finding a treatment for osteoporosis is essential for the development of modern medical care.

There are three types of treatments for osteoporosis and other bone diseases: autologous bone grafts, which use the patient's own healthy bone, allogeneic bone grafts, which use the same parts of bones from the different patients and artificial bone grafts [4]. Autologous bone grafts have the advantage of high biocompatibility and less rejection but also have disadvantages such as limited collection amount and the risk of secondary invasion due to two surgeries. On the other hand, allogeneic bone grafts use live or cadaveric donors bones of the same species and can have both osteoinductive and osteoconductive properties. However, there are disadvantages of associated with shorter usability span, and the risk of disease transmission or host immunogenic response occurring [5]. Therefore, artificial bones in block and granule form are used as

* Corresponding author at: Department of Applied Chemistry, School of Science and Technology, Meiji University, 1-1-1 Higashimita, Tama-ku, Kawasaki 214-8571, Kanagawa, Japan.
E-mail address: mamorua@meiji.ac.jp (M. Aizawa).
[1] These authors equally contributed to this work

https://doi.org/10.1016/j.bbiosy.2025.100107
Received 11 November 2024; Received in revised form 9 January 2025; Accepted 21 January 2025
Available online 26 January 2025
2666-5344/© 2025 The Author(s). Published by Elsevier Ltd. This is an open access article under the CC BY-NC-ND license (http://creativecommons.org/licenses/by-nc-nd/4.0/).

bone graft substitutes; however, they are difficult to shape and process [6]. To address these issues, we focused on paste-like artificial bones that could be injected with a syringe and adapted to different shapes of bone defects.

Polymethyl methacrylate (PMMA) bone cement is a paste-like artificial bone composed of pulverized polymers and monomers for easy shaping, widely used by orthopedic surgeons. However, PMMA does not degrade *in vivo*, and its high setting temperature can cause surrounding tissue necrosis [7]. Thus, alternative injection materials are needed. CPC is a paste-like artificial bone that sets at body temperature when mixed in the correct ratio of solid and liquid phases [8]. The current CPC consists of a two-component powder of acidic calcium hydrogen phosphate ($CaHPO_4$) and basic tetracalcium phosphate ($Ca_4O(PO_4)_2$), as proposed by Brown and Chow *et al* [9]. However, CPC ultimately forms hydroxyapatite ($Ca_{10}(PO_4)_6(OH)_2$; HAp), which remains in the body for a long time. In addition, hydroxyapatite does not have a compressive strength comparable to autogenous bone, which can lead to brittle fracture and the risk of revision surgery. Moreover, the acid-base reaction during cement paste setting may induce an inflammatory reaction around the tissue.

To address these issues, we developed a bioabsorbable chelate-setting β-tricalcium phosphate (β-TCP) cement based on the chelate-setting mechanism of inositol phosphate ($C_6H_6(OPO_3H_2)_6$; IP6) [10, 11]. Chelate-setting β-TCP cement, set with *in vivo* resorbable β-TCP in its main crystalline phase, utilizes the chelating ability of IP6, thus avoiding the risk of inflammation. The raw powders β-TCP and IP6 were ball-milled and surface-modified to obtain IP6/β-TCP powders. IP6 is found in wheat, rice, corn, and soybean and has strong chelating capability to calcium ions, similar to chelating compounds such as ethylenediaminetetraacetic acid (EDTA) [12]. Since higher bioresorbability is required for clinical applications of cement pastes, we prepared a chelate-setting IP6/β-TCP cement with bioresorbable poly (lactic-co-glycolic acid) (hereafter, "PLGA") particles [13]. We named this IP6/β-TCP cement with PLGA the organic/inorganic hybrid cement. The organic/inorganic hybrid cement containing PLGA particles showed higher bioresorbability than the cement without PLGA particles. However, adding PLGA particles prolongs the setting time of the cement pastes. Because clinical applications require more rapid bioresorption substitution properties, we prepared a new cement by adding calcium sulfate hemihydrate ($CaSO_4{\cdot}1/2H_2O$; CSH) to the hybrid cement [14]. In this organic/inorganic hybrid cement with simultaneous addition of CSH and PLGA particles, PLGA particle additions at 10 mass% and 20 mass% were evaluated, and it was found that adding PLGA particles improved the cement's bioresorbability [14]. Furthermore, the *in vivo* response of the hybrid cement was investigated in a rat calvaria defect model, which showed that bone was formed by the cooperation of osteoblasts and osteoclasts. The result shows that the hybrid cements are compatible with the bone remodeling cycles.

In this study, to optimize the amount of PLGA particles, we examined the effect of the amount of PLGA particles added to chelate-setting β-TCP cement's bioresorption and bone replacement properties, creating a fully resorbable paste-like artificial bone compatible with the bone remodeling cycle. Besides material characterization, *in vitro* and *in vivo* biological responses were assessed. *In vitro* evaluation clarified: i) cytotoxicity effects on cement specimens with various PLGA particle amounts using an indirect seeding method, and ii) relative cell proliferation rate determination using a direct seeding method. For *in vivo* evaluation, the resulting cement was implanted into pig tibias, with bone formation and material resorption rates quantitatively evaluating the hybrid cement's bioresorbability. Additionally, a commercially available HAp-based cement (Biopex®) was tested *in vivo* and compared with our hybrid cement.

2. Materials and methods

2.1. Preparation of the PLGA particles and their characterization

PLGA particles were prepared using a water-in-oil-in-water (w/o/w) double-emulsion solvent evaporation technique, following Habraken et al. [15]. Firstly, 3 g of polyvinyl alcohol (Fujifilm Wako Pure Chemical Industries Co. Ltd., Japan) was stirred in a beaker with 1000 cm^3 of pure water at 800 rpm and 50 °C for a week to create a 0.3 mass% polyvinyl alcohol (PVA) solution. Secondly, 1 g of PLGA (Sigma-Aldrich, average molecular weight (*Mw*) 34,000–54,000, lactic acid to glycolic acid ratio 50:50 [w/w]) powder was dissolved in 4 cm^3 of chloroform (Fujifilm Wako Pure Chemical Industries Co. Ltd., Japan) in a 50 cm^3 tube. To this tube, 0.5 cm^3 of pure water was added and vortexed for 90 s. Next, 6 cm^3 of a 0.3 mass% PVA solution was added to this 50 cm^3 tube containing PLGA and vortexed for 90 s. The contents of the 50 cm^3 tube were transferred to a 1000 cm^3 beaker containing 400 cm^3 of 2 mass% isopropyl alcohol (Fujifilm Wako Pure Chemical Industries Co. Ltd., Japan) while stirring, and another 394 cm^3 of 0.3 mass% PVA solution was slowly added to the 1000 cm^3 beaker. The suspension of PLGA, chloroform, and PVA solution was stirred at 700 rpm and 25 °C for 1 h, then left to stand and settle, after which the solution was decanted. The solution was centrifuged at 1000 rpm for 2 min, and the solution was aspirated. Finally, the PLGA particles were frozen and freeze-dried for 24 h.

PLGA particles were subsequently observed using a scanning electron microscope (SEM) (JSM6390LA, JEOL Ltd., Japan) at an accelerating voltage of 10 kV. For SEM observation, samples were coated with platinum using an ion-sputtering device. PLGA particle sizes were measured using a laser scattering particle size distribution analyzer (LA-300, Horiba Ltd., Japan), with median and mode sizes determined. Approximately 0.05 g of the prepared powder was ultrasonicated in 250 cm^3 of pure water for 3 min prior to measurement. The obtained PLGA particles were spherical, with median and mode diameters of 125.7 and 128.6 μm ($n = 7$), respectively, consistent with our previous reports [13, 14].

2.2. Preparation of the starting CPC powders

The starting CPC powders were prepared following the protocol in our previous report [10,11,13,14]. IP6 solutions (50 mass% phytic acid, Fujifilm Wako Pure Chemical Industries Co. Ltd., Japan) with concentrations of 3000 ppm were prepared using phytic acid and adjusted to pH 7.3 with NaOH solution (0.1 mol/dm^{-3}). Subsequently, 10 g of commercially available β-TCP powder (β-TCP-100, Taihei Chemical Industrial Co. Ltd., Japan) was placed in a 3000 ppm 40 cm^3 IP6 solution in a zirconia (ZrO_2) pot. The mixture was simultaneously ground and surface-modified with IP6 using a planetary ball mill (Pulverisette 6, Fritsch Japan Co. Ltd., Japan) in a ZrO_2 pot with 180 g of ZrO_2 beads (2 mm in diameter) at a rotation rate of 300 rpm for 3 h. After ball milling, the resulting slurry was filtered and freeze-dried for 24 h using a freeze-dryer (Free Zone, LABCONCO Corp., USA.) to yield β-TCP powders surface-modified with IP6 (hereafter, IP6/β-TCP powder). The resulting powders were sieved through a 200 mesh (150 μm), and the IP6/β-TCP powders were mixed with various amounts of CSH and PLGA particles using a V-shaped mixer (MC, Tsutsui Scientific Instruments Co. Ltd., Japan) for 5 min to produce a mixed powder.

As given in Table 1, the resulting powder mixtures are labeled by the amount of CSH and PLGA particles. According to a previous report [14], the optimum CSH addition is 20 mass%. The weight ratio of β-TCP to CSH, excluding the PLGA component, was set at 80:20 [mass%]. In this report, the presence or absence of CSH is indicated by "+" and "-". For instance, if PLGA particles are added to the IP6/β-TCP powder and CSH is present, the sample is labeled "CSH(+)/PLGA(x), x: mass%".

Table 1
Fabrication conditions of the cement specimens.

Sample	Composition/mass%			P/L ratio [w/v]
	IP6/-TCP	CSH	PLGA	
CSH(-)/PLGA(0)	100	0	0	1.0/0.9
CSH(-)/PLGA(10)	90	0	10	1.0/0.9
CSH(+)/PLGA(0)	80	20	0	1.0/0.7
CSH(+)/PLGA(5)	76	19	5	1.0/0.7
CSH(+)/PLGA(10)	72	18	10	1.0/0.7
CSH(+)/PLGA(20)	64	16	20	1.0/0.7

2.3. Preparation of the mixing liquid for the cement pastes

The mixing liquid was prepared following the protocol described in our previous reports [16,17]. Specifically, 2.5 g of disodium hydrogen phosphate (Na_2HPO_4), 1 g of sodium alginate ($(C_6H_7O_6Na)_n$), and 1.5 g of citric acid anhydride ($C_6H_8O_7$) were sequentially added to 95 g of purified water. The solution was adjusted to a pH of 7.0 using a NaOH solution (0.1 mol/dm^{-3}). All reagents (Wako Pure Chemical Industries, Co. Ltd., Japan) were used as received without further purification.

Disodium hydrogen phosphate promotes the transition of β-TCP to HAp, thereby enhancing compressive strength and reducing setting time [16]. Sodium alginate is expected to bind with Ca^{2+} ions in β-TCP, forming a gel to prevent disintegration [17]. Citric acid is expected to bind with Ca^{2+} ions in β-TCP, imparting a negative charge to the particles, thus improving dispersion by repelling the particles from each other [18].

2.4. Preparation of cement pastes and their properties

The cement pastes were prepared according to the methods outlined in our previous reports [13,14]. The prepared powder was mixed with the mixing liquid in an agate mortar using a rubber spatula for 2 min at the appropriate powder (P) to liquid (L) ratios of 1.0/0.9 and 1.0/0.7 [g/cm^3]. We have confirmed that the cement can be extruded as a paste with little or no load when it was filled into a syringe with an 18G needle.

The initial setting time (IST) was measured using a light Gillmore needle (113.4 g), in accordance with JIS T 0330-4. Following the preparation of the cement pastes, IST was measured at regular intervals until the cement pastes were fully set. The pastes were packed into plastic molds (8 mm in diameter and 2 mm in height). The Gillmore needle was gently lowered into the cement paste, and the end of the setting process was defined as the point at which the indentation completely disappeared.

2.5. Material properties of the cement specimens

Cement specimens for compressive strength (CS) measurements were prepared by casting the paste into cylindrical Teflon® molds (6 mm in diameter and 12 mm in height), which were then placed in an incubator (MIR-H163, PHC Holdings Corp.) at 37 °C and 100 % humidity for 24 h. The CS measurements were conducted on wet specimens immediately after removal from the incubator. A universal testing machine (AG-5KNXplus, Shimadzu Co. Ltd., Kyoto, Japan) was used for the CS testing. The crosshead speed was set at 0.5 mm·min^{-1}, and a 5 kN load cell was used. Three to four specimens were tested to calculate the average value and standard deviation (SD).

The crystalline phases of the cement specimens were identified using an X-ray diffractometer (XRD; Ultima IV, Rigaku Co. Ltd., Japan) with a CuKα radiation source. Data were collected over a 2θ range of 10°–50° with a step size of 0.02° and a counting time of 1.2 s per step. The crystalline phases were identified using the International Center for Diffraction Data database for β-TCP (#09-0169), HAp (#09-0432), and CSH (#43-605). The sample powder for XRD analysis was obtained by measuring the CS of the hardened cement specimens after 7 days of incubation, followed by grinding the crushed specimens in mortar.

The elements of the fracture surface in the cement specimens were analyzed using an energy-dispersive X-ray spectrometer (SEM-EDX; JFC-1500 ION SPUTTERING DEVICE, JEOL Co. Ltd., Tokyo, Japan) at an accelerating voltage of 15 kV. For SEM-EDX observation, the samples were sputter coated with platinum using an ion-sputtering device.

2.6. In vitro evaluation of the cement specimens

2.6.1. Preparation of the cell suspension

To examine the effects of cell proliferation on the cement specimens with added PLGA particles, two approaches were used: (i) a cytotoxicity test using an indirect seeding method and (ii) measuring the relative cell proliferation rate using a direct seeding method.

Cell culture studies were performed using the osteoblast-like cell line MC3T3-E1, derived from the cranial crown of neonatal C57BL/6 mice [19]. The cells were cultured in minimum essential medium alpha (α-MEM) supplemented with 10 vol% fetal bovine serum (FBS), referred to as α-MEM(+). The procedures for medium replacement and passaging are described below. MC3T3-E1 cells were cultured in 75 cm^2 flasks in an incubator at 37 °C, and 5 % CO_2. The medium was changed every other day, and the cells were passaged every 5 days, just before reaching confluence. The cells were treated with phosphate-buffered saline (PBS (-)) containing 0.1 mass% actinase, detached from the flasks, and neutralized with an equal volume of α-MEM(+). PBS(-) does not contain Ca^{2+} and Mg^{2+} ions. The suspension was then centrifuged (1000 rpm, 5 min), and the supernatant was discarded to resuspend the cells in fresh α-MEM(+). Cell suspensions were prepared to achieve a concentration of 5×10^4 cells/cm^{-3}, and 15 cm^3 of the suspension was seeded into new culture flasks.

2.6.2. Cytotoxicity evaluation using the indirect seeding method

The cement paste was filled into plastic molds (4 mm in diameter × 8 mm in height) and cured in an incubator (37 °C, 100 % relative humidity) for 24 h to obtain the cement specimens. These specimens were sterilized using an ethylene oxide gas sterilizer (CT-190C, Toho Plant Co. Ltd.). A cytotoxicity test was conducted using the Transwell® (CORNING) kit to evaluate the cytotoxicity of the cells and cement in co-culture. The cells were seeded in 12-well plates at a density of 6×10^4 cells/well and pre-cultured for one day. After 24 h, the medium was removed, and adherent cells were counted as the seeded (day 0) cells. Next, 1 cm^3 of medium was added to each well, and the cement specimens were placed in a Transwell® insert with 0.8 cm^3 of medium added. Cells cultured on polystyrene plates without Transwell® were used as controls. After placing the Transwell®, the cells were incubated for 1 or 3 days, and then the cells were removed and counted. For the 3 day culture samples, the medium was changed daily. Cell morphology was observed using an inverted microscope (CKX-41, Olympus Co. Ltd., Japan).

2.6.3. Cytotoxicity evaluation using the direct seeding method

Cement paste (~4.0 cm^3) was filled into a plastic mold with a pore diameter of 17 mm and a height of 2 mm, then cured in an incubator for 24 h to form cement specimens. These specimens were sterilized using ethylene oxide gas. The cement specimens were placed in 6-well plates, and 3 cm^3 of α-MEM(+) medium was added. After 24 h, the medium was removed, and 0.2 cm^3 of a cell suspension containing MC3T3-E1 cells at a density of 2.5×10^5 cells/well was seeded onto the cement specimens (17 mm in diameter and 2 mm in height), followed by incubation for 30 min at 37 °C, 5 % CO_2. An additional 3 cm^3 of medium was then added, and the specimens were incubated at 37 °C, 5 % CO_2 for 4 days, with the medium changed daily. For the samples incubated for 1 and 4 days, the medium was removed, and 3 cm^3 of fresh medium along with 0.3 cm^3 of MTT reagent was added and incubated for 4 h. After incubation, the medium with the reagent was removed, and the cells were dissolved

using dimethyl sulfoxide (DMSO). The number of cells in the dissolved solution was quantified by measuring the absorbance at 570 nm using a microplate reader (MULTISKAN FC, Thermo Fisher Co. Ltd., Japan). The equation derived from the calibration curve for MC3T3-E1 cell absorbance with the MTT reagent is shown in equation (2–6-1) below.

$$y = 1.51 \times 10^{-6}\, x \tag{2-6-1}$$

y: Absorbance [-]

x: Number of cells [cell]

Based on the obtained absorbance values, the cell count was determined using equation (2-6-1), and the relative cell proliferation rate was calculated using equation (2-6-2).

$$\text{Relative cell proliferation rate } [\%] = \frac{\log N_4 - \log N_1}{\log {N_4}^{Control} - \log {N_1}^{Control}} \times 100 \tag{2-6-2}$$

N_1: Day 1 cell count on the cement specimen

N_4: Day 4 cell count on the cement specimen $\log N_1^{Control}$: Day 1 cell count on the control $\log N_4^{Control}$: Day 4 cell count on the control

Morphological observation of cells cultured on cement specimens was performed using fluorescent staining. The cell nuclei were stained with DAPI, and the cytoskeleton was stained with phalloidin. Fluorescence-stained specimens were then observed using a fluorescence microscope (BZ-X700, KEYENCE Co. Ltd., Japan).

The medium from the 1, 2, 3, and 4-day incubation periods was collected daily, and the concentrations of Ca^{2+} and PO_4^{3-} ions in the medium were measured using inductively coupled plasma atomic emission spectroscopy (ICP-AES; SPS7800, SII Nanotechnology Corp. Ltd., Japan). For the control measurements, the collected medium was diluted 5-fold with ultrapure water, while the samples with cement specimens were diluted 20-fold.

2.7. *In vivo* evaluation of bioresorbable cement pastes using a pig miniature tibia defect model

In vivo evaluation of the cement pastes was conducted using a miniature pig tibia defect model, following protocols from our previous reports [13,14]. A female miniature pig weighing 40 kg was used to assess the bioresorbability of the set cement pastes and subsequent bone formation. The samples tested in this experiment included: i) Bio-pex®-R, ii) CSH(-)/PLGA(0), iii) CSH(+)/PLGA(5), iv) CSH(+)/PLGA (10), and v) CSH(+)/PLGA(20). The powders were sterilized using ethylene oxide gas, and the mixing liquid was filter-sterilized using a 0.20-μm filter (AZ-ONE Co. Ltd., Japan). The right tibias of the miniature pigs were exposed, and cylindrical defects 4.0 mm in diameter were drilled into the tibial epiphyses. On-site, the powder was mixed with the liquid for 2 min. The cement paste (0.15 cm^3) was filled into a plastic syringe, injected into the defect site, allowed to set *in vivo*, and then implanted for 12 weeks. Throughout the study, the pigs were fed a standard laboratory diet and given access to water. All surgical procedures were performed according to the Guidelines for the Animal Care and Use Committee of Meiji University (approval number: MUIACUC 2020-11). After 12 weeks of implantation, the pigs were sacrificed, and their tibias were harvested for analysis.

For histological observation, the freshly isolated tibias were fixed in 70 % ethanol, and non-decalcified polished sections were prepared after immersing the tibias in Villanueva bone (VB) stain solution. Polished sections approximately 50 μm thick were then observed using optical and fluorescence microscopes. Villanueva bone staining enables the identification of the calcification stage of the bone under both normal light and fluorescence. Under normal light, analogous bone stains reddish-purple, hypocalcified bone stains light orange, calcified bone stains light purple, and cytoplasmic spicules stain blue-purple. In fluorescence, analogous bone appears red, hypocalcified bone orange, calcified bone green, and cytosol is seen in a shadowy pattern. To evaluate the bioresorbability of the implanted cement, the area of the defect and the remaining cement area were measured from fluorescence images using image analysis software (WinROOF, Mitani Corp. Ltd., Japan) to determine the absorption rate. Similarly, the bone-forming area was measured to assess whether the balance between bioresorbability and bone-forming capacity was favorable. Additionally, the cement resorption-replacement rate was calculated by comparing the material resorption area with the bone formation area. The absorption rate, bone formation rate, and cement resorption-replacement rate were determined using Equations (2–7-1, 2–7-2, and 2–7-3).

$$\text{CPC} - \text{resorption rate } (\%) = \frac{\{\text{Bone defects area } (\text{mm}^2) - \text{Remaining cements area } (\text{mm}^2)\}}{\text{Bone defects area } (\text{mm}^2)} \times 100 \tag{2-7-1}$$

$$\text{Bone} - \text{formation rate } (\%) = \frac{\text{Newly} - \text{formed bone area } (\text{mm}^2)}{\text{Bone defects area } (\text{mm}^2)} \times 100 \tag{2-7-2}$$

$$\text{CPC resorption} - \text{replacement rate } (\%) = \frac{\text{Newly} - \text{formed bone area } (\text{mm}^2)}{\text{CPC resorption area } (\text{mm}^2)} \times 100 \tag{2-7-3}$$

2.8. *Statistical analysis*

Quantitative data were presented as means ± standard deviations. Differences between the two groups were analyzed by Student's *t*-test. $p < 0.05$ was considered statistically significant. Microsoft Excel for Microsoft 365 (Microsoft Co., One Microsoft Way, Redmond, WA 98,052-7329, USA) was used for calculations.

3. Results

3.1. *Properties of the CPC pastes*

Fig. 1 (a) shows the IST of the cement pastes. The IST of CSH(-)/PLGA (10), where only PLGA particles were added to the IP6/β-TCP powder, was approximately 30 min, which was longer than that of CSH(-)/PLGA (0), the cement paste containing only β-TCP/IP6 powder. The IST of the CSH(+)/PLGA(0) cement paste, in which only CSH was added to the IP6/β-TCP powder, was shorter than that of CSH(-)/PLGA(0). Furthermore, in the CPCs with simultaneous addition of PLGA particles and CSH, it was observed that the IST decreased, similar to the case where only CSH was added. However, adding 20 mass% PLGA particles to the powder mixed with CSH prolonged the IST. In this measurement, CSH (+)/PLGA(5) was newly evaluated, and it was confirmed that the IST was reduced, as in the case of adding only CSH. The addition of PLGA particles up to 10 mass% had minimal effect on the IST of the cement pastes.

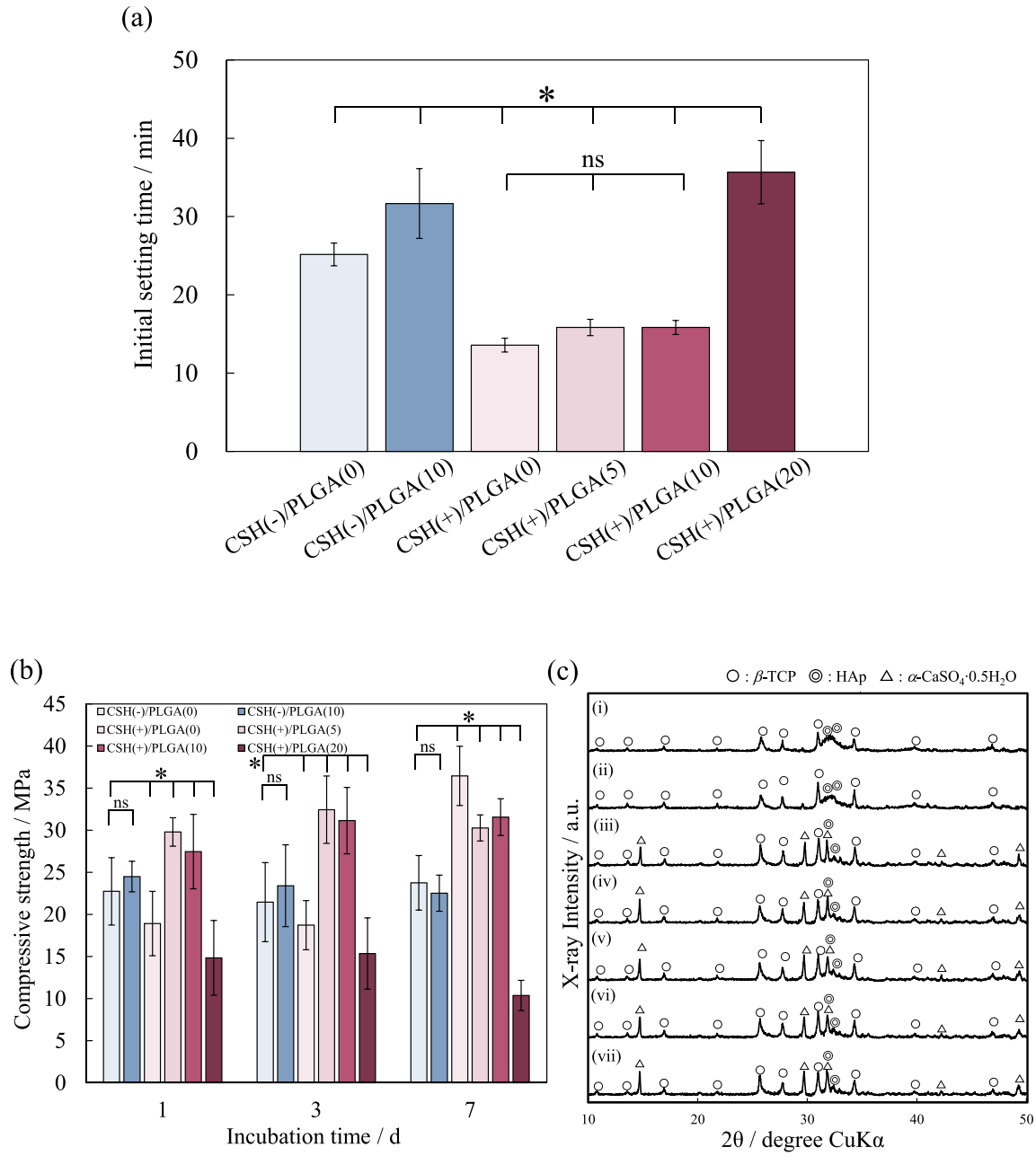

Fig. 1. Material properties of the cement specimens: (a) Initial setting time of the cement pastes; (b) Compressive strength of the cement specimens; (c) X-ray diffractometer (XRD) patterns of the cement specimens: (i) CSH(-)/PLGA(0), (ii) CSH(-)/PLGA(10), (iii) CSH(+)/PLGA(0), (iv) CSH(+)/PLGA(5), (v) CSH(+)/PLGA (10), (vi) CSH(+)/PLGA(15), (vii) CSH(+)/PLGA(20). (Error bars represent standard deviation [SD], $n = 3$–6, ns: no significant difference, *: $p < 0.05$).

3.2. Material properties of the CPC cement

Fig. 1 (b) shows the CS of the cement specimens with the simultaneous addition of PLGA particles and CSH. The CS of the cement specimens tended to increase with the duration of incubation. After 7 days of incubation, the CS of the specimens with both CSH and PLGA particles exceeded 30 MPa. However, the addition of 20 mass% PLGA particles to the mixture resulted in a significant decrease in CS.

Fig. 1 (c) presents the XRD pattern of the cement specimens with the simultaneous addition of CSH and PLGA particles. The sample powder for XRD measurement was obtained by grinding the cement specimens in a mortar after measuring the CS of the specimens incubated for 7 days. The main crystalline phase of the CSH(-)/PLGA(0) and CSH(-)/PLGA (10) cement specimens, which lacked CSH, was β-TCP, with a small amount of HAp present. In contrast, the crystalline phases of all the cement specimens containing CSH were mixtures of β-TCP, HAp, and CSH. No differences in the crystalline phases were observed with varying amounts of PLGA particles added.

Fig. 2 (a) shows SEM images of the cement specimens with the simultaneous addition of PLGA particles and CSH after 7 days of incubation. In the specimens with added PLGA particles, particles ranging from 50−100 μm in size were observed.

Fig. 2 (b) presents the results of the elemental analysis of the fracture surface of the CSH(+)/PLGA(10) cement after 7 days of incubation. The elements Ca, P, Na, and S were identified. As seen in the SEM images, spherical particles measuring 50−100 μm were observed. In the elemental mapping, the spherical particles contained few Ca, P, and S elements, suggesting they are PLGA particles. The distribution of Ca, P, and S elements throughout the cement section was uniform.

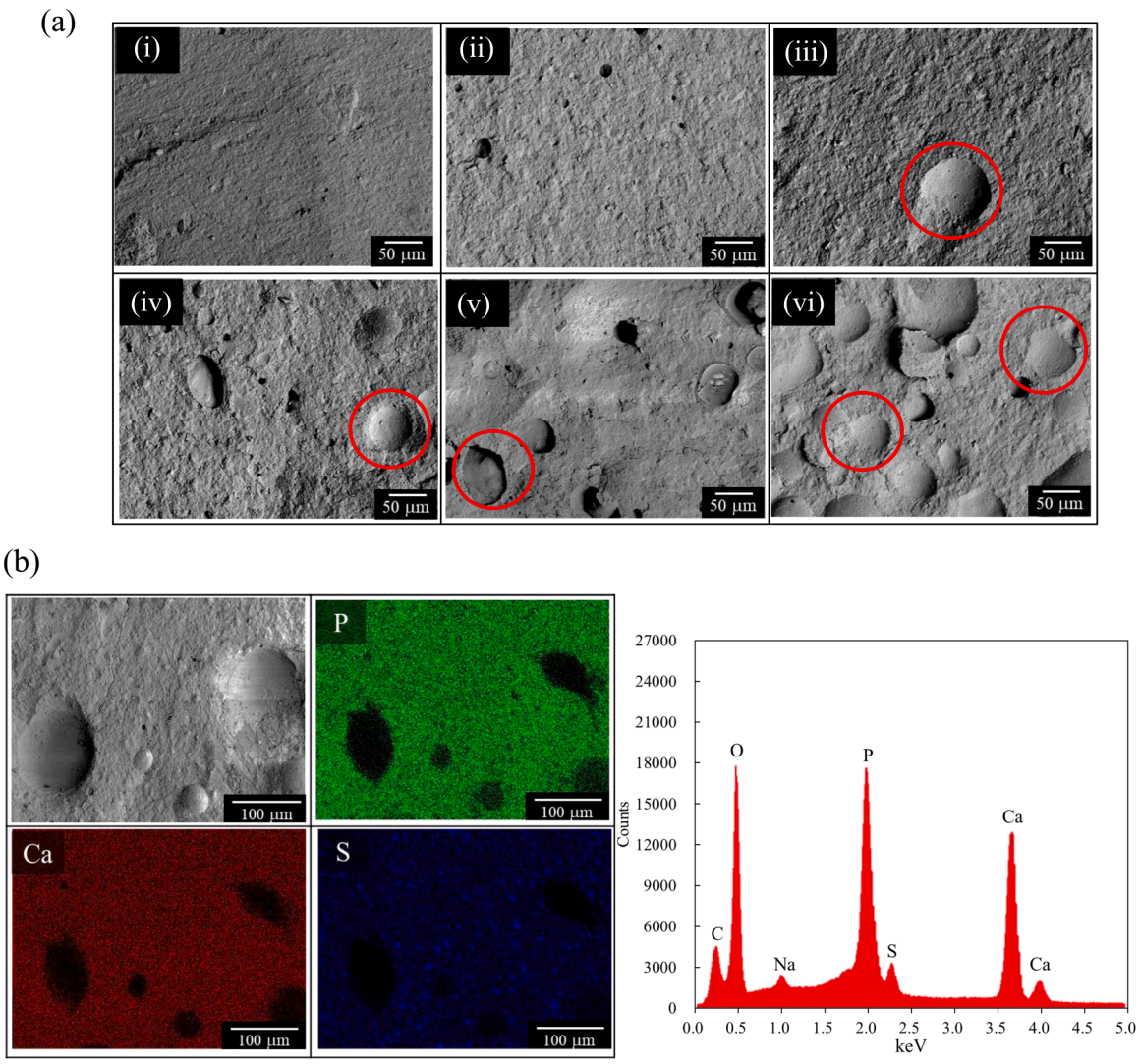

Fig. 2. Morphological observation of the cement specimens: (a) SEM image of the fracture surface of the cement specimens after 7 days of incubation: (i) CSH (-)/PLGA(0), (ii) CSH(+)/PLGA(0), (iii) CSH(+)/PLGA(5), (iv) CSH(+)/PLGA(10), (v) CSH(+)/PLGA(15), (vi) CSH(+)/PLGA(20) (red circle: place where PLGA particles originally existed); (b) Energy-dispersive X-ray spectrometry (EDX) spectrum of CSH(+)/PLGA(10).

3.3. In vitro evaluation of the cement specimens

Fig. 3 (a) shows the cell count results from the cytotoxicity test using Transwell®. Cells exposed to cement specimens in the insert exhibited similar growth to the control group. These results suggest that the cement specimens prepared in this study were not cytotoxic, regardless of the amount of PLGA particles added.

Fig. 3 (b) shows the cell morphology after 3 days of incubation in the cytotoxicity test. All samples displayed a similar level of elongated cells as observed in the control group. Therefore, the results suggest that the organic/inorganic hybrid cement with the simultaneous addition of CSH and PLGA particles does not affect cytotoxicity.

Fig. 4 shows the number of cells determined by the MTT assay, along with the relative cell proliferation rate. Fig. 4 (a) indicates that cell growth occurred from day 1 to day 4 in all samples, including the control. Fig. 4 (b) reveals differences in relative growth rates between the CSH(-) specimens (without CSH) and the CSH(+) specimens (with CSH). The CSH(-) specimens exhibited a significant decrease in relative growth rate compared to the control, while the CSH(+) specimens displayed a relative growth rate at least as high as the control.

Fig. 4 (c) presents the morphological observations from fluorescence staining, which showed an extended cytoskeleton in the control, CSH (-)/PLGA(0), and CSH(+)/PLGA(5) samples. The results of the Ca^{2+} and PO_4^{3-} ion concentration measurements in the medium after 4 days of cell culture (Fig. 4 (d) and (e)) indicate that the CSH(-) specimens had lower Ca^{2+} ion concentrations and higher PO_4^{3-} ion concentrations compared to the control. In contrast, the CSH(+) specimens showed higher Ca^{2+} ion concentrations and lower PO_4^{3-} ion concentrations relative to the control.

3.4. In vivo evaluation of cement specimens using a pig tibia model

Fig. 5 illustrates the histological evaluation of the cement specimens in pig tibia using Villanueva bone staining. Fig. 5 (a) and (b) shows that the CSH(+)/PLGA(5) and CSH(+)/PLGA(10) specimens, which included PLGA particles, demonstrated material degradation compared to Biopex® and CSH(-)/PLGA(0). Calcified bone was observed in all samples. Additionally, osteogenesis was detected within the material in the CSH(+)/PLGA(5) and CSH(+)/PLGA(10) specimens with PLGA particles. Fig. 5 (c) shows that Biopex® and CSH(-)/PLGA(0) had lower absorption rates compared to the cement specimens containing PLGA particles. The material resorption rate increased with the amount of PLGA particles added, with CSH(+)/PLGA(20) exhibiting the highest resorption rate among the examined CPCs. Fig. 5 (d) shows that CSH (+)/PLGA(5) had the highest bone formation rate, approximately 33%.

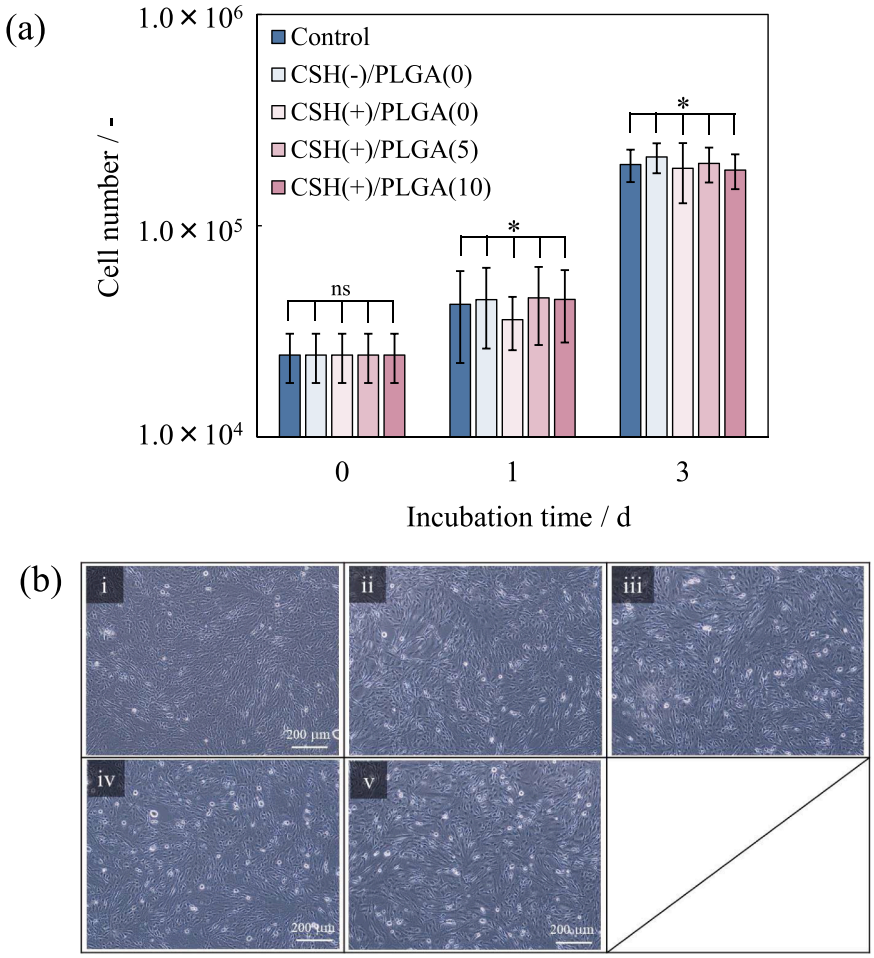

Fig. 3. Cytotoxicity test of the cement using Transwell®: (a) Cell proliferation of MC3T3-E1 cells cultured with a Transwell® in 12-well plates after 1 and 3 days of incubation; (b) Cell morphology of MC3T3-E1 cells cultured with a Transwell® in 12-well plates after 3 days of incubation: (i) control, (ii) CSH(-)/PLGA(0), (iii) CSH (+)/PLGA(0), (iv) CSH(+)/PLGA(5), (v) CSH(+)/PLGA(10). (Error bars represent standard deviation [SD], $n = 3$–6, ns: no significant difference, *: $p < 0.05$).

The bone formation rates for Biopex® and CSH(-)/PLGA(0) were below 10 %, while CSH(-)/PLGA(10) and CSH(+)/PLGA(10) had bone formation rates of approximately 23 %, and CSH(+)/PLGA(20) had a rate of about 18 %. Fig. 5 (e) indicates that CSH(+)/PLGA(5) had the highest absorption-substitution rate, followed by CSH(+)/PLGA(10). The absorption-substitution rate of CSH(+)/PLGA(20) was similar to that of CSH(-)/PLGA(0), which did not contain PLGA particles.

4. Discussion

We have developed the CPC that sets with bioresorbable β-TCP as the main crystalline phase, utilizing the chelating ability of IP6 [10,11]. Additionally, we successfully created a fully resorbable CPC hybridized with poly(lactic-co-glycolic acid) (PLGA) [13] and calcium sulfate hemihydrate (CSH) [14]. However, the optimal amount of PLGA particles to be added to the hybrid cement for optimal *in vivo* reactions has not yet been determined. In this study, we examined the effect of the amount of PLGA particles on the bioresorption and bone replacement properties of chelate-setting β-TCP cement, aiming to develop a fully resorbable, paste-like artificial bone compatible with the bone remodeling cycle.

In the organic/inorganic hybrid cements with simultaneous addition of CSH and PLGA particles, the addition of 10 and 20 mass% PLGA particles was previously evaluated, showing that the inclusion of PLGA improved bioresorbability [14]. To optimize the amount of PLGA particles, we introduced a new sample with 5 mass% PLGA particles and examined its material properties, as well as its *in vitro* and *in vivo* responses.

The IST of the cement paste is a crucial material property, with approximately 15 min considered sufficient for clinical applications [20]. For the samples where PLGA particles and CSH were added simultaneously, it was confirmed that the IST was around 15 min, except for CSH(+)/PLGA(20). Therefore, the addition of up to 10 mass% PLGA particles is considered to have minimal impact on the IST of the cement pastes.

The CS of approximately 30 MPa was observed in the CSH/PLGA(5) and CSH/PLGA(10) specimens, which exceeds the CS of human vertebrae (1.5–7.8 MPa) [21]. This result aligns with our previous study [14], which demonstrated that the addition of CSH effectively improves cement strength. However, adding 20 mass% PLGA particles to the cement mixture resulted in a significant decrease in CS. As noted in our previous reports [13,14], this may be due to the inhibition of the setting reaction between the primary component β-TCP and the mixing liquid when the amount of PLGA particles increases, leading to a reduction in CS. X-ray diffraction patterns revealed that the crystalline phase of the cement specimens was a mixture of β-TCP and HAp, regardless of the presence of PLGA particles.

All cement specimens containing CSH exhibited mixed phases of β-TCP, HAp, and CSH, indicating that the addition of PLGA particles and CSH has little effect on the crystalline phase of the cement.

SEM images revealed spherical particles of 50–100 μm in size in the cement specimens with added PLGA particles. Previous reports [13,14]

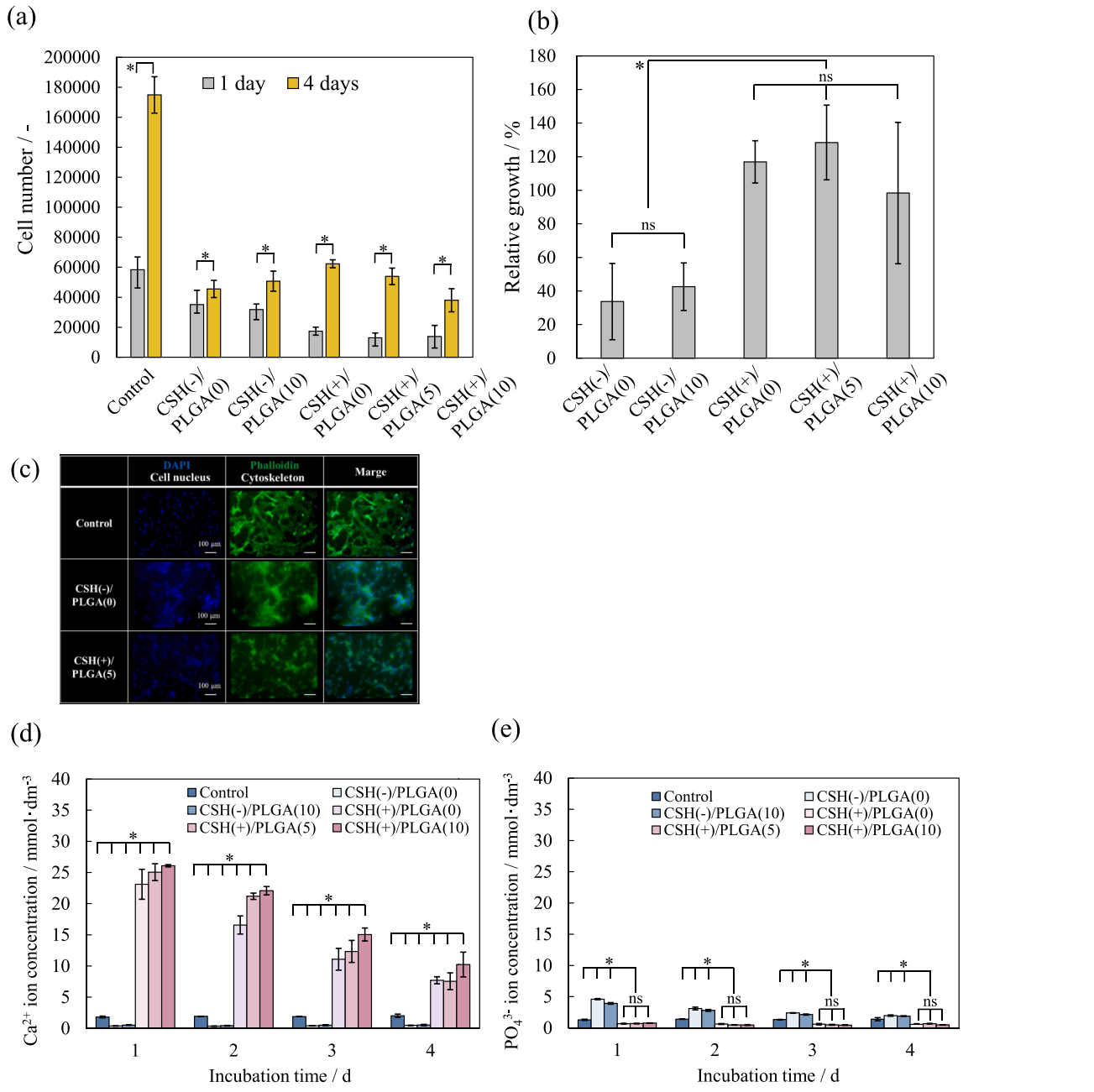

Fig. 4. Cell relative proliferation test using MTT reagent: (a) Cell proliferation of MC3T3-E1 cells in 6-well plates after 1 and 4 days of incubation; (b) Cell morphology of MC3T3-E1 cells cultured with a Transwell® in 12-well plates after 3 days of incubation: (i) control, (ii) CSH(-)/PLGA(0), (iii) CSH(+)/PLGA(0), (iv) CSH(+)/PLGA(5), (v) CSH(+)/PLGA(10); (c) Cell morphology by fluorescent staining; (d) Ca^{2+} ion concentration in the medium; (e) $PO4^{3-}$ ion concentration in the medium. (Error bars represent standard deviation [SD], $n = 3$–6, ns: no significant difference, *: $p < 0.05$).

confirmed that the PLGA particles prepared in this study are spherical, with a particle size of approximately 100 μm. In the specimens with both PLGA particles and CSH, PLGA particles were observed within the cement, suggesting that the particles dissolve during *in vivo* placement, resulting in a porous cement structure. In CSH(+)/PLGA(10), elements such as Ca and P, likely derived from β-TCP, Na from disodium hydrogen phosphate and sodium alginate in the mixing liquid, and S from CSH were identified. Elemental mapping showed the presence of Ca, P, and S within the spherical particles (50−100 μm), likely indicating the presence of PLGA particles in the mixture. The elements Ca, P, Na, and S were uniformly distributed throughout the cement, suggesting thorough mixing of the cement powder.

The cytotoxicity test using the indirect seeding method with Transwell® showed that all cement specimens exhibited a similar number of proliferating and viable cells as the control. These results suggest that variations in the number of PLGA particles added have minimal effect on the cytotoxicity of the cement specimens. In the test measuring the relative cell proliferation rate using the MTT reagent by the direct seeding method, it was confirmed that cells proliferated from day 1 to day 4 in all samples, including the control. However, the relative growth rate of the CSH(-) specimens was significantly lower than that of the control, while the CSH(+) specimens showed a growth rate at least as high as that of the control. This difference in growth rates may be attributed to the concentration of Ca^{2+} and PO_4^{3-} ions in the medium. The CSH(-) specimens had lower Ca^{2+} ion concentrations and higher PO_4^{3-} ion concentrations compared to the control. In contrast, the CSH(+) specimens exhibited higher Ca^{2+} ion concentrations and lower PO_4^{3-} ion concentrations than the control. Elevated Ca^{2+} ion concentrations are

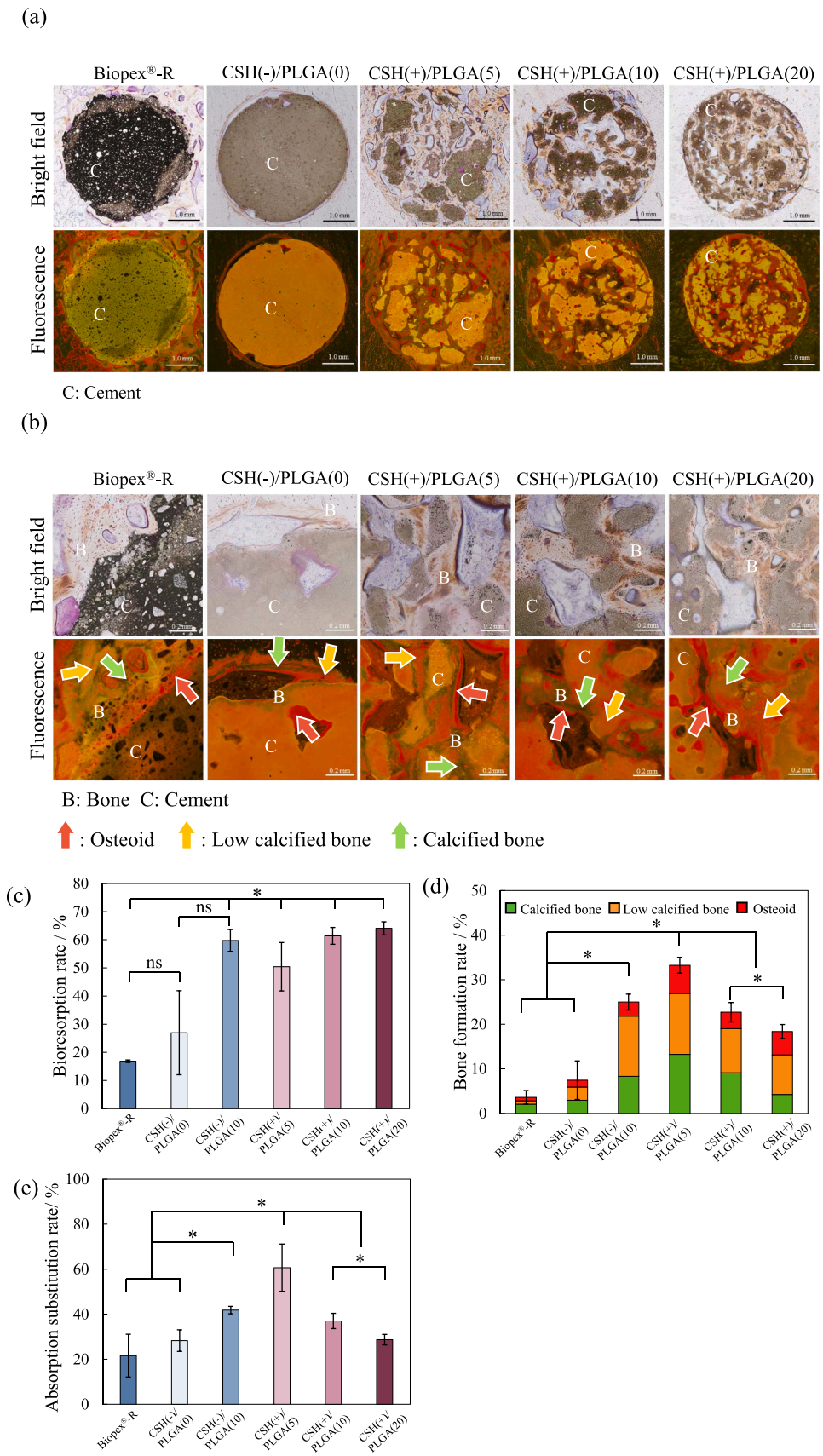

Fig. 5. Histological evaluation of the cement with Villanueva bone staining on the basis of a pig tibia defect model: (a) Low magnification (overview); (b) High-magnification image of (a) (C: remaining cement specimens, B: newly-formed bone); (c) Bioresorption rate of the cement specimens; (d) Bone formation rate of cement specimens; (e) Absorption-substitution rate of the cement specimens. (Error bars represent standard deviation [SD], $n = 3$–4, ns: no significant difference, *: $p < 0.05$).

known to accelerate osteoblast proliferation [22], while PO_4^{3-} ion concentrations above 3 mM can induce cell apoptosis [23]. The low Ca^{2+} and high PO_4^{3-} ion concentrations in the CSH(-) specimens likely inhibited osteoblast proliferation, resulting in a lower relative proliferation rate compared to the control.

Results from an *in vivo* evaluation of the cement pastes using a pig tibia defect model showed that the addition of PLGA particles to the cement enhanced material degradation compared to β-TCP cement and commercial HAp-based cements (Fig. 5(a) and (b)). Fig. 5(d) shows that CSH(+)/PLGA(5) exhibited the highest bone formation rate, approximately 33 %, among the examined CPCs. The percentage of low-calcified bone and osteoid was significantly higher in the cement with PLGA particles than in β-TCP cement or commercial HAp-based cements, indicating that the entire bone tissue was oriented toward new bone formation. Fig. 5 (e) shows that CSH(+)/PLGA(5) also had the highest absorption-substitution ratio, followed by CSH(+)/PLGA(10). The material absorption rate increased with the amount of PLGA particles added, with significant material absorption observed in some areas when 10 and 20 mass% PLGA particles were added, compared to the sample with 5 mass% PLGA. The cement with 5 mass% PLGA particles had the highest bone formation rate, as compared to the 10 and 20 mass % sample, likely because non-bone tissue infiltrated the areas with higher PLGA content, hindering bone formation (Fig. 5(c)). In particular, the cement with 20 mass% PLGA particles had a reduced resorption-replacement ratio due to significant material resorption, which allowed non-bone tissue to invade, thereby preventing osteogenesis. These findings confirm that the organic/inorganic hybrid cement with 5 mass% PLGA particles promotes the most favorable bone formation and has a good resorption–replacement rate. Our previous report [14] has also shown osteoblast and osteoclast activity in a rat calvaria defect model in the hybrid cement. The CPCs developed in this study represent a promising new bone replacement material that is well-suited to the bone remodeling cycle.

5. Conclusion

A fully-resorption replacement paste-like organic/inorganic artificial bone compatible with the bone remodeling cycle was successfully developed by the simultaneous addition of CSH and PLGA particles in appropriate ratios. The new organic/inorganic hybrid cement demonstrated a CS of approximately 30 MPa and set in about 15 min, making it easy to handle in clinical applications. *In vitro* evaluation using the indirect seeding method showed that cell proliferation in all cement specimens was nearly equivalent to that in the control. The *in vivo* evaluation results indicated that the highest bone formation rate, along with optimal material resorption and replacement, occurred when 5 mass% PLGA particles were added, demonstrating a favorable balance between material resorption and bone formation.

Based on these findings, the optimal amount of PLGA particles in the CSH and PLGA particle-enhanced β-TCP cement is 5 mass%, which provides excellent material properties and compatibility with bone remodeling cycles. This formulation is expected to serve as a fully resorbable, organic-inorganic/hybrid cement with favorable characteristics for bone replacement and compatibility with the bone remodeling process.

CRediT authorship contribution statement

Yuki Kamaya: Writing – original draft, Visualization, Validation, Software, Methodology, Investigation, Formal analysis, Data curation. **Shiori Kato:** Validation, Methodology, Investigation. **Kazuaki Nakano:** Writing – review & editing, Supervision, Resources. **Masaki Nagaya:** Writing – review & editing, Supervision, Resources. **Hiroshi Nagashima:** Writing – review & editing, Supervision, Resources. **Mamoru Aizawa:** Writing – review & editing, Supervision, Resources, Project administration, Funding acquisition, Conceptualization.

Declaration of competing interest

The authors declare that they have no known competing financial interests or personal relationships that could have appeared to influence the work reported in this paper.

Acknowledgments

This research was supported by a research grant from Meiji University to the Meiji University International Institute for Materials with Life Functions.

Data availability

Data will be made available on request.

References

[1] Gibon E, Lu LY, Nathan K, Goodman SB. Inflammation, ageing, and bone regeneration. J Orthop Transl 2017;10:28–35. https://doi.org/10.1016/j.jot.2017.04.002.
[2] Padilla Colón CJ, Molina-Vicenty IL, Frontera-Rodríguez M, García-Ferré A, Rivera BP, Cintrón-Vélez G, Frontera-Rodríguez S. Muscle and bone mass loss in the elderly Population: Advances in diagnosis and treatment. J Biomed (Syd) 2018;3:40–9. https://doi.org/10.7150/jbm.23390.
[3] Salari N, Ghasemi H, Mohammadi L, Behzadi MH, Rabieenia E, Shohaimi S, Mohammadi M. The global prevalence of osteoporosis in the world: a comprehensive systematic review and meta analysis. J Orthop Surg Res 2021;16:609. https://doi.org/10.1186/s13018-021-02772-0.
[4] Damien CJ, Parsons JR. Bone graft and Bone graft substitutes: a review of current technology and applications. J Appl Biomater 1991;2:187–208. https://doi.org/10.1002/jab.770020307.
[5] Ciszyński M, Dominiak S, Dominiak M, Gedrange T, Hadzik J. Allogenic bone graft in dentistry: aA review of current trends and developments. Int J Mol Sci 2023;24:16598. https://doi.org/10.3390/ijms242316598.
[6] Tsuru K, Sugiura Y, Ishikawa K. Nanobioceramics for Healthcare Applications, 6. London: World Scientific Publishing Europe Ltd; 2017. p. 151–86.
[7] Webb JC, Spencer RF. The role of polymethylmethacrylate bone cement in modern orthopaedic surgery. J Bone Joint Surg Br 2007;89:851–7. https://doi.org/10.1302/0301-620X.89B7.
[8] Liu H, Li H, Cheng W, Yang Y, Zhu M, Zhou C. Novel injectable calcium phosphate/chitosan composites for bone substitute materials. Acta Biomater 2006;2:557–65. https://doi.org/10.1016/j.actbio.2006.03.007.
[9] Brown WE, Chow LC. Dental resptorative cement pastes. US Patent. 1985. No. US4518430A.
[10] Takahashi S, Konishi T, Nishiyama K, Mizumoto M, Honda M, Horiguchi Y, Oribe K, Aizawa M. , Fabrication of novel bioresorbable β-tricalcium phosphate cement on the basis of chelate-setting mechanism of inositol phosphate and its evaluation. J Ceram Soc Jpn 2011;119:35–42. https://doi.org/10.2109/jcersj2.119.35.
[11] Konishi T, Takahashi S, Zhuang Z, Nagata K, Mizumoto M, Honda M, Takeuchi Y, Matsunari H, Nagashima H, Aizawa M. Biodegradable β-tricalcium phosphate cement with anti-washout property based on chelate-setting mechanism of inositol phosphate. J Mater Sci Mater Med 2013;24:1383–94. https://doi.org/10.1007/s10856-013-4903-8.
[12] Dao TH. Polyvalent cation effects on myo-inositol hexakis dihydrogenphosphate enzymatic dephosphorylation in dairy wastewater. J Environ Qual 2003;32:694–701. https://doi.org/10.2134/jeq2003.6940.
[13] Ando A, Kamikura M, Takeoka Y, Rikukawa M, Nakano K, Nagaya M, Nagashima H, Aizawa M. Bioresorbable porous β-tricalcium phosphate chelate-setting cements with poly(lactic-co-glycolic acid) particles as pore-forming agent: fabrication, material properties, cytotoxicity, and *in vivo* evaluation. Sci Technol Adv Mater 2021;22:511–21. https://doi.org/10.1080/14686996.2021.1936628.
[14] Kamaya Y, Ando A, Suzuki K, Nakano K, Nagaya M, Nagashima H, Aizawa M. Development of paste-like organic/inorganic artificial bones compatible with bone remodeling cycles, consisting of β-tricalcium phosphate, calcium sulfate hemihydrate, and poly(lactic-co-glycolic acid) particles. New J Chem 2024;48:8545–55. https://doi.org/10.1039/d3nj05820d.
[15] Habraken WJ, Wolke JG, Mikos AG, Jansen JA. Injectable PLGA microsphere/calcium phosphate cements: physical properties and degradation characteristics. J Biomater Sci Polym Ed 2006;17:1057–74. https://doi.org/10.1163/156856206778366004.
[16] Nagata K, Fujioka K, Konishi T, Honda M, Nagaya M, Nagashima H, Aizawa M. Evaluation of resistance to fragmentation of injectable calcium-phosphate cement paste using X-ray microcomputed tomography. J. Ceram. Soc. Jpn 2017;125:1–6. https://doi.org/10.2109/jcersj2.16199.
[17] Miyamoto Y, Ishikawa K, Takechi M, Yuasa M, Kon M, Nagayama M, Asaoka K. Non-decay type fast-setting calcium phosphate cement: setting behaviour in calf serum and its tissue response. Biomaterials 1996;17:1429–35. https://doi.org/10.1016/0142-9612(96)87286-3.

[18] Sarda S, Fernández E, Nilsson M, Balcells M, Planell JA. Kinetic study of citric acid influence on calcium phosphate bone cements as water-reducing agent. J Biomed Mater Res 2002;61:653–9. https://doi.org/10.1002/jbm.10264.
[19] Sudo H, Kodama HA, Amagai Y, Yamamoto S. In vitro differentiation and calcification in a new clonal osteogenic cell line derived from newborn mouse calvaria. J Cell Biol 1983;96:191–8. https://doi.org/10.1083/jcb.96.1.191.
[20] Khairoun I, Boltong MG, Driessens FC, Planell JA. Limited compliance of some apatitic calcium phosphate bone cements with clinical requirements. J Mater Sci Mater Med 1998;9:667–71. https://doi.org/10.1023/a:1008939710282.
[21] Mosekilde L, Mosekilde L. Normal vertebral body size and compressive strength: relations to age and to vertebral and iliac trabecular bone compressive strength. Bone 1986;7:207–12. https://doi.org/10.1016/8756-3282(86)90019-0.
[22] Atif AR, Pujari-Palmer M, Tenje M, Mestres G. A microfluidics-based method for culturing osteoblasts on biomimetic hydroxyapatite. Acta Biomater 2021;127:327–37. https://doi.org/10.1016/j.actbio.2021.03.046.
[23] Adams CS, Mansfield K, Perlot RL, Shapiro IM. Matrix regulation of skeletal cell apoptosis. Role of calcium and phosphate ions. J Biol Chem 2001;276:20316–22. https://doi.org/10.1074/jbc.M006492200.